

Operation Experience of the Wendelstein 7-X High Temperature Superconductor Current Leads

Reinhard Heller, Holger Bau, Michael Nagel, and Thomas Rummel

Abstract— The fusion device Wendelstein 7-X (W7-X) is a modular stellarator which went into operation at the Greifswald branch of the Max-Planck-Institut für Plasmaphysik in December 2015. The main component is the superconducting magnet system which consists of 50 nonplanar and 20 planar coils, 14 high temperature superconductor (HTS) current leads (CLs), and more than 100 superconducting bus bars. The HTS CLs with a maximum current of 18.2 kA were constructed, tested and delivered by the Karlsruhe Institute of Technology (KIT). In the first plasma physics campaign the nonplanar coils were operated with a maximum current of 12.4 kA while the planar coils were energized up to 4.9 kA. The paper describes the performance of the HTS CLs during plasma operation. A comparison to the acceptance test results performed after the construction of the CLs at KIT will be presented.

Index Terms— Current Lead, Fusion Magnets, High Temperature Superconductors.

I. INTRODUCTION

THE hot plasma of the stellarator fusion experiment Wendelstein 7-X (W7-X) is confined within a magnetic cage which is generated by a superconducting magnet system consisting of 50 Non Planar Coils (NPC) and 20 Planar Coils (PC). HTS CLs connect the cold superconducting bus bars with current feeders at ambient temperature outside the cryostat. The coils and their support structures are cooled with supercritical helium at 3.9 K. The cooling is provided by a helium-refrigerator with an equivalent cooling power of 7 kW at 4.5 K.

Commissioning and the first operational phase of the stellarator Wendelstein 7-X (W7-X) have been accomplished successfully [1][2]. The first helium plasma was achieved on 10th of December 2015 followed by the first hydrogen plasma in February 2016. The plasma is confined by a magnetic field of 2.5 T on the plasma axis created by the superconducting magnet system.

II. DESCRIPTION OF SUPERCONDUCTING COIL AND AUXILIARY SYSTEMS

The superconducting magnet of W7-X consists of 50 non-planar (NPC1 to NPC5) and 20 planar (PC1 and PC2) coils arranged in five modules of a pentagon symmetry. Each module consists of five different NPCs and 2 different PCs. All coils of each type are connected in series via superconducting

bus bars (BB) to two HTS CLs. This arrangement guarantees the five-fold symmetry for the plasma, as all coils of the same type have the same current, but gives also large flexibility of the magnet configuration. Details of the magnet system can be found in [3].

The HTS CLs were designed, constructed and tested by KIT [4],[5]. The maximum current of the CLs is 18.2 kA and the nominal current is 14 kA. A conventional Cu heat exchanger (HX) is used between room temperature and 60 K. The Cu HX consists of a central conductor with fins and it is cooled with 50 K He. The HX is connected to a HTS module consisting of a thin stainless steel dodecagon with copper end caps and Bi-2223/AgAu tapes arranged in stacks and soldered in grooves milled on the outer surface which covers the temperature range between 60 K and 4.5 K and is cooled by heat conduction towards the cold end of the CLs.

Each current lead (CL) is instrumented with temperature sensors and voltage taps to control its operation and evaluate its performance, e.g., the temperature profile or the voltage along the HTS module in case of a quench. Fig. 1 shows a sketch of a CL with selected sensors relevant for the analysis presented in this paper, e.g. sensors to measure the temperature at the warm end of the HTS module $T_{100\%HTS}$, the He inlet temperature to the HX $T_{He\ in}$ and the voltage drop along the HTS module including the copper end caps U_{HTS} . At the room temperature end the CL pair is connected via a multi-contact-plug and short length copper braids to water-cooled Aluminum bus bars leading to 20 kA power supplies. Differential pressure sensors are installed at the He inlet and outlet to determine the pressure drop along the HX. The He mass flow rate through the HX is measured by a mass flow meter (FI-CL) at the outlet. The heat load \dot{Q}_{cold} at the cold end of the CLs is composed of the static heat load via conduction through the

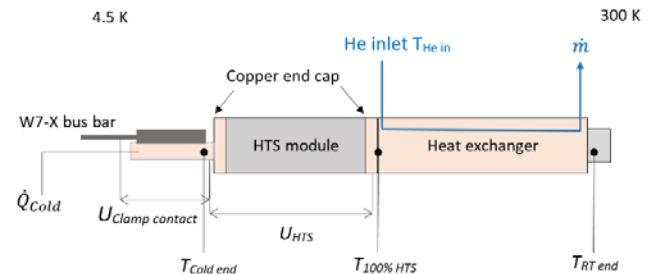


Fig. 1. Sketch of the W7-X CL instrumentation.

Manuscript receipt and acceptance dates will be inserted here.

R. Heller is with the Karlsruhe Institute of Technology KIT, Institute for Technical Physics, Karlsruhe, Germany (e-mail: reinhard.heller@kit.edu), H. Bau,

M. Nagel and T. Rummel are with Max Planck Institut für Plasmaphysik, Teilinstitut Greifswald, Greifswald, Germany

CL and the resistive loss of the cold end contact. The latter one consists of the contact resistance at the cold end of the HTS module and the clamp contact resistance between the CL and the bus bar. \dot{Q}_{cold} is removed by the helium flowing in the bus bar and in the contact cooling (CC). Fig. 2 shows the HTS CL cooling circuits.

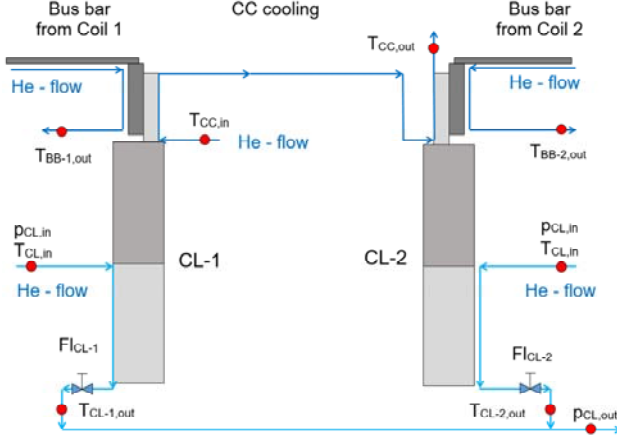


Fig. 2. HTS current lead cooling circuits and He sensors.

For the determination of the operation performance of the current leads, the He temperatures, pressures and mass flow rates are needed. In W7-X the following information is available:

1. CL cooling: He inlet pressure $p_{He,CL-in}$, He temperature $T_{He,in}$ and He mass flow rate \dot{m}_{CL} for each individual CL;
2. BB cooling: He inlet pressure $p_{He,coil-in}$, He temperature $T_{He,coil-in}$, He pressure drop $dp_{He,coil}$, and He mass flow rate \dot{m}_{coil} of the whole coil cooling. The BB is connected in series to the innermost or outermost layer of a coil. The outlet of the inner coil layers are equipped with temperature sensors $T_{coil,out}$. It was decided to use the sensors of that coil located close to the CL as representative for the inlet temperature of the BB cooling. Each CL has its individual BB cooling. There is some uncertainty in the knowledge of the He mass flow rate of the BB cooling as there are 6 times 50 cooling circuits for NPC and 3 times 20 cooling circuits for PC resulting in 360 parallel cooling channels. There is a $\pm 20\%$ spread in the helium mass flow rate of the individual channels due to fluctuation of the helium void fraction and differences in the length of the different layers [6];
3. CC cooling: He inlet pressure $p_{He,CC-in}$, He temperature $T_{He,CC-in}$, He pressure drop $dp_{He,case}$, and He mass flow rate \dot{m}_{case} . The casings of all superconducting coils are cooled with a He-flow using a parallel cooling scheme. The casing outlet flow of seven planar coils is then used to provide the cold contact cooling of seven CL-pairs (one coil casing outlet is used for one CL-pair). The CC cooling of the two CL's of each CL pair is connected in series, i.e. seven cooling circuits are realized. The He pressure drop $dp_{He,casing}$ is the pressure drop over the cooling circuit (coil casing and CC cooling), the He mass flow rate \dot{m}_{case} is the mass flow of one coil casing.

Details of the cooling system of W7-X and its performance can be found in [7].

For the performance evaluation, a full day current operation of the whole coil system during plasma operation has been selected. In the following, the results are presented and discussed.

III. HTS CURRENT LEAD PERFORMANCE DURING PLASMA OPERATION

Fig. 3 shows the CL temperatures $T_{Cold\ end}$, $T_{100\%HTS}$ and $T_{RT\ end}$, the He inlet temperature $T_{He\ in}$, and the current of the seven coil circuits I_{NPC} and I_{PC} during the whole day as a function of time. Without current operation, the $T_{100\%HTS}$ is kept 5 - 15 K higher compared to the temperature during current operation due to the reduction of the mass flow of the He-cooling which lowers the RT heat load and avoids wet RT-ends. Before current operation, $T_{100\%HTS}$ is lowered by increasing the mass flow to be prepared for joule heating. The He mass flow rates during night and during current operation are plotted in Fig. 4; here the PC have a much lower helium mass flow rate than the NPC because the current is much lower. The temperature change of $T_{100\%HTS}$ can be seen in Fig. 3.

The voltages across the clamp contact $U_{Clamp\ contact}$ and along the HTS module U_{HTS} which include both copper end caps were taken to calculate the resistances R_{HTS} and R_{CC} during current operation. The results are shown in Fig. 5 where R_{HTS} , R_{CC} , and $T_{100\%HTS}$ are plotted as a function of the CL number. The average values are $\langle R_{HTS} \rangle = (17.91 \pm 1.52)$ n Ω and $\langle R_{CC} \rangle = (3.22 \pm 0.35)$ n Ω respectively while $\langle T_{100\%HTS} \rangle = (56.9 \pm 0.6)$ K.

The total losses are measured with the enthalpy change of the helium flowing in the BB and CC circuits. Due to the fact that for the contact cooling the sum of both CLs of the same current circuit is measured it is not possible to determine the losses of each individual CL. The pressure at the outlet of the manifold (inlet pressure minus pressure drop) has been used for enthalpy calculations as this is closer to the pressure at the CLs.

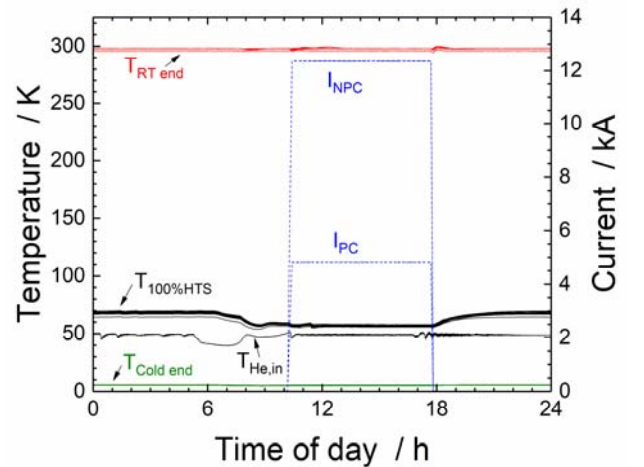


Fig. 3. CL temperatures $T_{Cold\ end}$, $T_{100\%HTS}$ and $T_{RT\ end}$, He inlet temperature $T_{He\ in}$, and the current of the seven coil circuits I_{NPC} and I_{PC} during the whole day as a function of time.

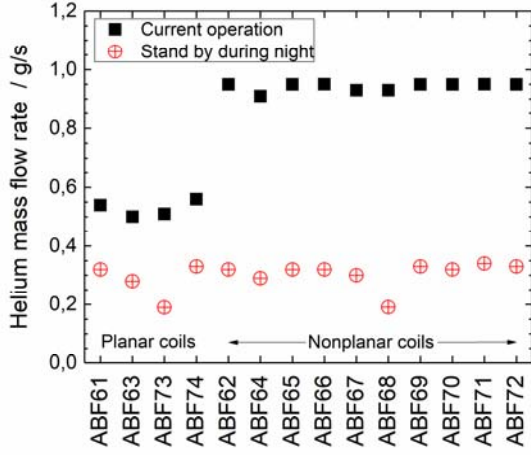


Fig. 4. He mass flow rates during night (crossed circles) and during current operation (full rectangles) as a function of the CL number.

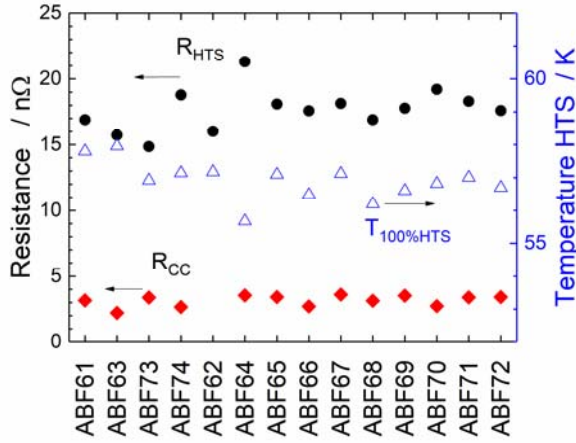


Fig. 5. Electrical resistance R_{HTS} (full circles) and R_{CC} (full diamond) and the temperature $T_{100\%HTS}$ (open triangle) as a function of the CL number.

Fig. 6 shows the helium temperatures of the bus bar and contact cooling for the CLs during current operation. It is important to mention that in case of the contact cooling circuits, the two CL which belong together are connected in series with sensors located at the inlet of one CL and at the outlet of the other CL, i.e., no data for the single CL are available. The error bar given is the calibration error of the sensors. But it has to be noted that the measurement error is much larger because all temperature sensors within the W7-X machine are arranged in blocks mounted on the He cooling pipes [7] and the absolute error depends on the local conditions as conduction and radiation heat loss and heat transfer between the helium flowing inside the pipes and the sensor block [8]. This can be seen for example in Fig. 6a where the BB outlet temperatures of the CL ABF66 and ABF67 are much lower than the other ones. In Fig. 6b, the CC outlet temperature of ABF63 is much higher and of ABF70 it is much lower than the others. It should also be noted that the helium temperatures show no difference prior to plasma operation (i.e., without current) and during current operation.

Table I summarizes the main parameters for the loss calculations and in Table II the resultant losses are presented. Due to malfunction of the outlet temperature sensor of the contact cooling of coil circuit PC1 and that of the mass flow rate of bus bar cooling of PC2 and no measurable difference in the case cooling temperature of NPC1, those CL circuits cannot be used and the related losses cannot be determined. Using the results of the four remaining CL circuits, the resultant average resistance was calculated from the resistive losses leading to $\langle R_{coldend} \rangle = (8.02 \pm 2.45 \pm 1.61) \text{ n}\Omega$. The first error denotes the statistical error whereas the second error is related to the $\pm 20\%$ spread in the helium mass flow for the 360 double layers of the coils. If subtracting the clamp contact resistance R_{CC} one gets $(4.80 \pm 2.48 \pm 1.61) \text{ n}\Omega$ as contribution of the copper end cap of the HTS module which is in fair agreement to $5.88 \text{ n}\Omega$ estimated from the total resistance of the HTS-module.

The average losses before starting current operation are estimated to be $(7.03 \pm 3.43) \text{ W}$. The results obtained so far are compared to those from the acceptance test [9]. Table III summarizes this.

TABLE I
MAIN PARAMETERS FOR THE LOSS CALCULATIONS

Parameter	Unit	0 kA	I_{op}
$T_{He,in}$ in Coil	K	3.85	3.85
$T_{He,in}$ in BB	K	4.05	4.08
$T_{He,out}$ in BB	K	4.91	4.98
$T_{He,in}$ in CC	K	4.26	4.27
$T_{He,out}$ in CC	K	4.86	4.93
Total He flow coil circuit	g/s	200	200
Total He flow case circuit	g/s	300	300
Av. He flow in coil circuit	g/s	0.555	0.555
Av. He flow in case circuit	g/s	4.29	4.29
$p_{He,in}$ in coil circuit	bar	3.64	3.63
$p_{He,in}$ in case circuit	bar	3.34	3.33
Δp in coil circuit	bar	0.39	0.38
Δp in case circuit	bar	0.04	0.03

TABLE II: CALCULATED LOSSES BEFORE (0) AND DURING CURRENT OPERATION (I)

Coil circuit	Coil current [kA]	BB cooling $\dot{Q}_{BB,0}$ [W]	BB cooling $\dot{Q}_{BB,I}$ [W]	CC cooling $\dot{Q}_{CC,0}$ [W]	CC cooling $\dot{Q}_{CC,I}$ [W]	Sum \dot{Q}_0 [W]	Sum \dot{Q}_I [W]
PC1	4.849	5.95	6.29	77.44	83.13	N/A	N/A
PC2	N/A	N/A	N/A	7.89	8.14	N/A	N/A
NPC3	12.364	6.55	7.04	11.84	13.75	18.39	20.79
NPC5		3.01	3.28	12.96	14.61	15.97	17.89
NPC4		3.17	3.55	14.80	17.95	17.97	21.5
NPC1		4.89	5.54	0.94	0.94	N/A	N/A
NPC2		4.47	4.97	-0.56	0.90	3.91	5.87

TABLE III: COMPARISON BETWEEN RESULTS DURING PLASMA OPERATION AND ACCEPTANCE TEST

Parameter	Unit	Plasma operation	Acceptance test
R_{HTS}	n Ω	(17.91 ± 1.52)	(18.43 ± 0.40)
\dot{Q}_0	W	(7.03 ± 3.43)	$(2.15 \pm 0.05 \pm 1)$

While the total resistance along the HTS module estimated from the data taken during plasma operation are in nice agreement to the results obtained during the acceptance tests, the average losses measured before starting the current operation are much larger than the zero current losses measured for each

current lead at KIT. But here it has to be considered that the losses measured during the acceptance tests did not include background losses from the test arrangement which were determined to be in the order of 12 – 15 W whereas in W7-X other sources of losses – beside those from the current leads – are not known and could therefore not be subtracted.

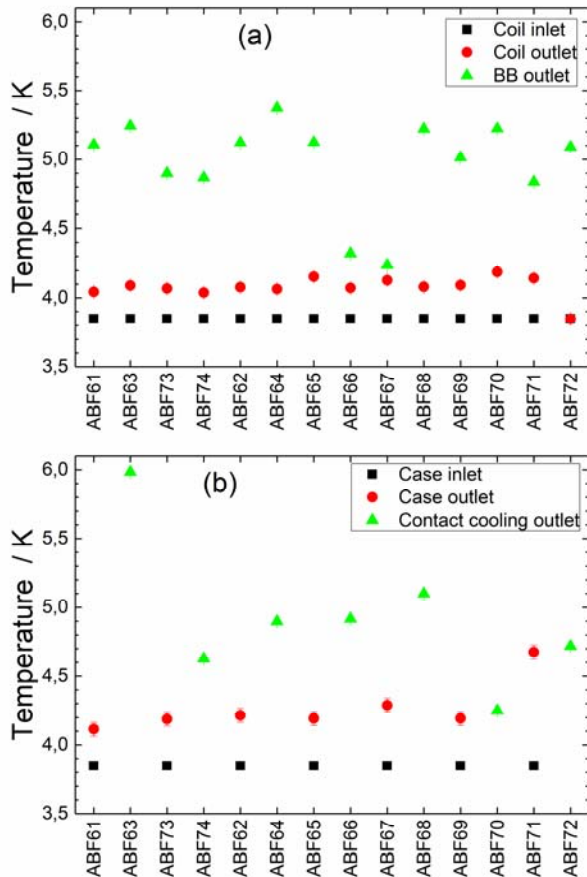


Fig. 6. He temperatures of the bus bar (a) and contact (b) cooling for the CLs during;

In Fig. 7 the He mass flow rates through the HX as a function of current are shown and compared to the acceptance test data. The agreement is very good.

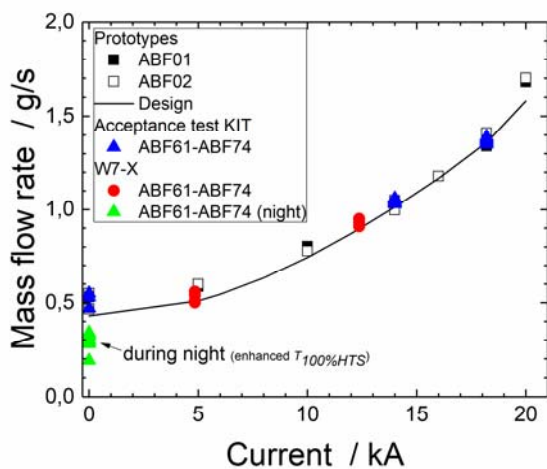


Fig. 7. He mass flow rates through the HX as a function of current are shown and compared to the acceptance test data.

The measured temperatures at the CLs were compared to the expected temperature profiles calculated with the code CURLEAD [10] for the different operations stand-by during night, zero current before plasma operation and current operation (12.364 kA for NPC and 4.821 kA for PC). For these 4 cases, average temperatures for the 10 NPC and 4 PC CLs were calculated which are shown in Fig. 8. The agreement is good which confirms that the CLs behave as expected.

As mentioned above, the scattering of the temperature signals as shown in Fig. 6 reflects not only the different behavior of the single CL but also the uncertainty in the temperature measurements and the uncertain He mass flow distribution for the different cooling circuits. A comparison of the average temperature calculated from temperatures measured with blocks at the coil pipes (inlet / outlet) shows a good agreement with temperatures measured directly in the He-flow in the valve box of the feed and return header (4.10 K compared to 4.18 K [6]). The temperature difference measured by the same sensor is considered to be more precise than the absolute value. The same general behavior is expected for the sensors mounted in the CL contact cooling circuit. Therefore, average values are considered as more significant than those of single measurements. So, the general behavior of the CL within the W7-X cryostat can be summarized as given in Table IV and exemplarily shown in Figure 9. From this it is concluded that the cold contact cooling takes approx. 2/3 of the heat load as

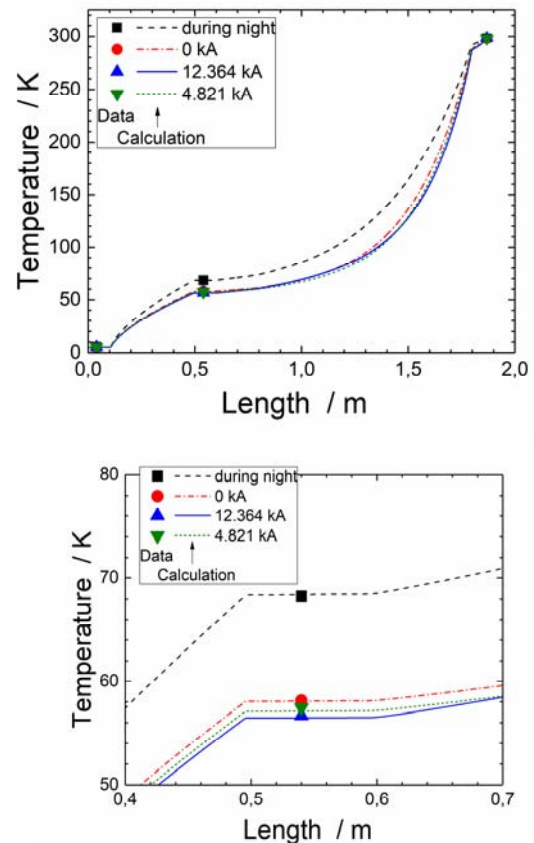


Fig. 8. Measured and calculated temperature profiles for different operations: during night, before plasma operation and during current operation. Top: whole temperature profile, Bottom: temperature profiles at the HTS-HX interface area.

the mass flow is a factor three larger than the bus bar cooling flow.

TABLE IV: AVERAGE TEMPERATURES AT CL COOLING

Parameter	Temperature	Comment
Bus bar cooling	$\Delta T = 1.0$ K	Temperature difference between outlet and inlet
	$\Delta T_{\text{outlet}} = 0.08$ K	Temperature difference with / without current
Cold contact cooling	$\Delta T = 0.60$ K	Temperature difference between outlet and inlet
	$\Delta T_{\text{outlet}} = 0.08$ K	Temperature difference with / without current
CL(cold end)	$T = 5.27$ K	
	$\Delta T = 0.25$ K	Temperature difference with / without current

Overnight, i.e. between the daily experimental campaigns, the He- temperature for the coil inlet is increased from 3.9 K to 4.4 K and the mass flow rate for CL cooling is reduced causing the warm end temperature at the HTS ($T_{\text{HTS},100\%}$) to increase by 5 - 15 K. Consequently, the heat load at the cold end of a single CL increases by about 2 W.

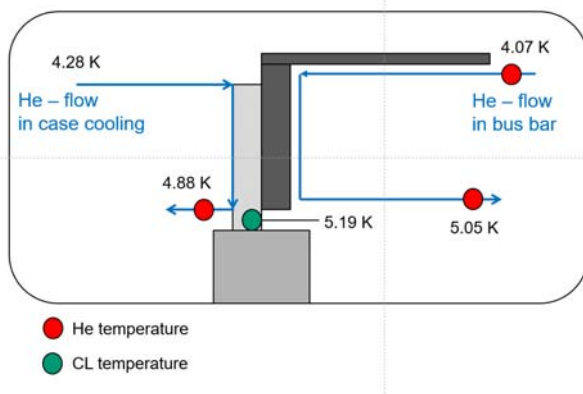


Fig. 9. Overview of temperatures at the cold end of the CL.

IV. SUMMARY

The modular stellarator Wendelstein 7-X (W7-X) went into operation at the Greifswald branch of the Max-Planck-Institut für Plasmaphysik in December 2015. The performance of the 14 HTS CL which connect the 70 superconducting coils to the power supplies have been investigated by taking data during plasma operation with a maximum current of the coils of 12.4 kA. As characteristic parameters which determine the performance of the leads the He mass flow rate required for the CL heat exchangers, the resistances along the HTS modules, and the losses at the cold end of the CL were chosen and the results were compared to those obtained during the acceptance tests of the CL at KIT. As a general result, it can be said that the leads could be operated safely and behave as expected from the design and validated in the acceptance tests.

During the following experimental campaigns, the coil currents will be increased up to the maximum design value allowing further investigation of the current lead performance.

ACKNOWLEDGMENT

Part of this work has been carried out within the framework of the EUROfusion Consortium and has received funding from the Euratom research and training programme 2014-2018 under grant agreement No 633053. The views and opinions expressed herein do not necessarily reflect those of the European Commission.

REFERENCES

- [1] Rummel T, Nagel M, Bykov V, Birus D, Carls A, Dhard C P, Köster E, Mönnich T, Riße K, Schneider M, Bosch H S, and the W7-X team, "Commissioning Results of the Superconducting Magnet System of Wendelstein 7-X", *IEEE Trans. Appl. Supercond.* vol. 27, no. 44200307, 2017.
- [2] Bosch H S, Brakel E, Braeuer T, Bykov V, van Eeten P, Feist J H, Füllenbach F, Gasparotto M, Grote H, Klinger T, Laqua H, Nagel M, Naujoks D, Otte M, Risse K, Rummel T, Schacht J, Spring A, Sunn Pedersen T, Vilbrandt R, Wegener L, Werner A, Wolf R C, Baldzuhn J, Biedermann C, Braune H, Burhenn R, Hirsch M, Höfel U, Knauer J, Kornejew P, Marsen S, Stange T, Trimino Mora H, W7-X Team., "Final integration, commissioning and start of the Wendelstein 7-X stellarator operation", *Nucl. Fusion* vol. 57, 116015, 2017.
- [3] Rummel T, Riße K, Ehrke G, Rummel K, John A, Mönnich T, Buscher K P, Fietz W H, Heller R, Neubauer O, and Panin A, "The Superconducting Magnet System for the Stellarator Wendelstein 7-X", *IEEE Trans. Plasma Science* vol. 40, no. 3)pp. 769-776, 2012.
- [4] Heller R, Drotziger S, Fietz W H, Fink S, Heiduk M, Kienzler A, Lange C, Lietzow R, Möhring T, Rohr P, Rummel T, Mönnich T, and Buscher K P, "Test Results of the High Temperature Superconductor Prototype Current Leads for Wendelstein 7-X", *IEEE Trans. Appl. Supercond.* vol. 21 no. 3pp. 1062-1065, 2011.
- [5] Heller R, Buscher K P, Drotziger S, Fietz W H, Kienzler A, Lietzow R, Mönnich T, Richter T, Rummel T, Urbach E, "Status of series production and test of the HTS current leads for Wendelstein 7-X", *Fusion Engineering and Design* vol. 88 pp. 1482- 1485, 2013.
- [6] Maix R K, Bagnato V, Fricke M, Heyn K, Kluck T, Lange F, Riße K, Sborchia C, Valle N, "Design, Production and QA Test Results of the NbTi CIC Conductors for the W7-X Magnet System", *Journal of Physics: Conference Series* vol. 43 pp. 753-758, 2006.
- [7] Nagel M, Dhard C P, Bau H, Bosch H S, Meyer U, Raatz S, Risse K, Rummel T, "Cryogenic commissioning, cool down and first magnet operation of Wendelstein 7-X", *IOP Conf. Series: Materials Science and Engineering* vol. 171 012050, 2017.
- [8] Müller R, Süßer M, "Comparison of cryogenic temperature sensor installation inside or outside the piping", *AIP Conference Proceedings* vol. 1218 pp. 1641-1646, 2010.
- [9] Drotziger S, Buscher K P, Fietz W H, Heiduk M, Heller R, Hollik M, Lange C, Lietzow R, Moennich T, Richter T, Rummel T, "Overview of results from Wendelstein-7-X HTS current lead testing", *Fusion Engineering and Design* vol. 88 pp. 1585- 1588, 2013.
- [10] Heller R, "Numerical calculation of current leads for fusion magnets", *KfK-4608*, Karlsruhe, 1989